Article

Discovery Medicine 2025; 37(200): 2006–2018
https://doi.org/10.24976/Discov.Med.202537200.172

ASAP3 Inhibits RAC1 Activation and Mediates Mitochondria-Endoplasmic Reticulum Crosstalk to Attenuate Myocardial Ischemia-Reperfusion Injury

Ziyang Yu[1], Yirong Teng[2], Hongbo Yang[3], Yudi Wang[1], Xichen Li[1], Lei Feng[4], Wenbo Xu[5], Yanping Li[1,*], Yinglu Hao[1,*]

[1]Department of Cardiology, The 6th Affiliated Hospital of Kunming Medical University, The People's Hospital of Yuxi City, 653199 Yuxi, Yunnan, China
[2]Department of General Practice, The 6th Affiliated Hospital of Kunming Medical University, The People's Hospital of Yuxi City, 653199 Yuxi, Yunnan, China
[3]Department of Cardiology, Fuwai Yunnan Hospital, Chinese Academy of Medical Sciences, 650102 Kunming, Yunnan, China
[4]Department of Laboratory, Yan'an Hospital of Kunming City, 650051 Kunming, Yunnan, China
[5]Department of Laboratory, The 6th Affiliated Hospital of Kunming Medical University, The People's Hospital of Yuxi City, 653199 Yuxi, Yunnan, China
*Correspondence: yuxiliyanping@aliyun.com (Yanping Li); yingluhao@aliyun.com (Yinglu Hao)
Submitted: 25 April 2025 Revised: 21 July 2025 Accepted: 28 July 2025 Published: 20 September 2025

Background: Myocardial injury induced by ischemia-reperfusion (I/R) remains a major barrier to improved clinical outcomes and continues to compromise human health. Adenosine diphosphate-ribosylation factor GTPase-activating protein (ArfGAP) with homology 3 (SH3) domain, ankyrin repeat, and pleckstrin homology (PH) domain-containing protein 3 (ASAP3) is a key regulator involved in cytoskeletal remodeling, membrane dynamics, and signal transduction. Its potential role in the pathogenesis of myocardial I/R injury, however, remains unclear. This study aims to elucidate the function of ASAP3 in myocardial I/R injury.

Methods: A hypoxia-reperfusion (H/R) injury model was established in H9c2 cells. The expression of ASAP3 and ras-related C3 botulinum toxin substrate 1 (RAC1) was modulated by transfection. Cell viability and apoptosis were subsequently assessed. Additionally, intracellular Ca^{2+} accumulation, mitochondrial reactive oxygen species (ROS) production, mitochondrial membrane potential, and adenosine triphosphate (ATP) levels were evaluated. Endoplasmic reticulum (ER) stress and mitochondria-ER crosstalk were also investigated. Co-immunoprecipitation (Co-IP) experiments were conducted to verify the ASAP3-RAC1 interaction.

Results: ASAP3 expression was significantly downregulated following H/R injury ($p < 0.01$), concomitant with reduced cell viability and increased apoptosis in H9c2 cells ($p < 0.01$). Overexpression of ASAP3 significantly improved cell viability and decreased apoptosis under H/R conditions ($p < 0.01$). Furthermore, ASAP3 overexpression reduced intracellular Ca^{2+} accumulation ($p < 0.01$), preserved mitochondrial and ER function as evidenced by increased JC-1 and ATP levels, and reduced ROS production and ER stress markers ($p < 0.01$). Co-IP experiments confirmed a physical interaction between ASAP3 and RAC1, suggesting a possible direct regulatory mechanism. Notably, RAC1 overexpression abolished the protective effects of ASAP3 ($p < 0.01$), highlighting an antagonistic interplay between these proteins.

Conclusions: Overexpression of ASAP3 in cells subjected to H/R injury inhibits RAC1 activation and facilitates mitochondria-endoplasmic reticulum crosstalk, thereby alleviating cardiomyocyte injury.

Keywords: ASAP3; RAC1; myocardial ischemia-reperfusion injury; apoptosis

Introduction

The implementation of reperfusion therapies, including percutaneous coronary intervention (PCI) and coronary artery bypass grafting (CABG), has greatly advanced the management of acute myocardial infarction [1]. Nonetheless, myocardial injury following reperfusion remains an inevitable consequence [2]. Ischemia/reperfusion (I/R) injury can induce extensive cardiomyocyte death, subsequently leading to myocardial fibrosis and remodeling, which contribute to the progressive deterioration in cardiac function [3,4]. Over time, this condition elevates the risk of heart failure. Studies indicate that I/R injury constitutes approximately 30% to 50% of the overall myocardial damage observed in patients experiencing acute myocardial infarction [5,6]. Despite the exploration of various clinical strategies and pharmacological agents aimed at mitigating this injury, effective interventions remain limited, rendering the pre-

vention and management of I/R injury a notable challenge in both clinical and scientific contexts [7]. I/R injury is primarily driven by oxidative damage, calcium dysregulation, and disturbances in mitochondrial and endoplasmic reticulum function [8]. Targeted therapeutic approaches encompass pharmacological treatments (such as calcium channel blockers, antioxidants, and β-blockers) and mechanical protective strategies (primarily involving transient ischemia in distal limbs to activate systemic protective mechanisms and reduce myocardial I/R damage) [9]. Although existing therapies can partially alleviate I/R injury, numerous limitations persist, particularly the lack of precise interventions targeting critical molecular pathways associated with I/R damage [10]. Consequently, investigating the underlying mechanisms of myocardial I/R injury is essential, not only for elucidating the intricate pathological processes involved in managing acute myocardial infarction but also in advancing the optimization of therapeutic strategies, the development of cardioprotective agents, the application of stem cell therapies, and related areas.

The endoplasmic reticulum (ER) and mitochondria are recognized as critical organelles implicated in I/R injury, significantly influencing cellular survival and apoptosis [11,12]. Through close physical and functional interactions, these organelles establish the mitochondria-associated endoplasmic reticulum membrane (MAM) [13]. The MAM consists of lipids, various proteins, and calcium transporters that are essential for energy metabolism, calcium homeostasis, and lipid metabolism in cardiomyocytes [14]. Notably, dysfunction of the MAM has been observed in cardiomyocytes subjected to I/R injury, suggesting that impaired MAM function contributes to the mechanisms driving I/R injury development [15]. ArfGAP with homology 3 (SH3) domain, ankyrin repeat, and pleckstrin homology (PH) domain-containing protein 3 (ASAP3), an adenosine diphosphate-ribosylation factor GTPase-activating protein (ArfGAP), also referred to as development and differentiation-enhancing factor-like 1 (DDEFL1) or adenosine diphosphate-ribosylation factor 6 GTPase-activating protein (ACAP4), plays a pivotal role in regulating cytoskeletal dynamics, membrane trafficking, and signal transduction [16]. Research indicates that ArfGAP influences cell morphology and migration through the modulation of Rho family GTPases, which are integral to actin remodeling [17]. Additionally, ArfGAP regulates endocytosis, membrane trafficking, and intracellular membrane remodeling through modulation of Arf6 activity [18]. Recent studies increasingly suggest a potential link between ArfGAP and mitochondrial function, calcium homeostasis, and apoptosis, leading to the hypothesis that ASAP3 may also regulate MAM function [19]. It has been indicated that ArfGAP family proteins may significantly contribute to various cardiovascular diseases, leading to increased interest in ASAP3 in the context of myocardial I/R injury [20]. To date, most studies on ASAP3 have focused on its involvement in cancer cell motility and invasive behavior [21]. Moreover, ras-related C3 botulinum toxin substrate 1 (RAC1), a member of the Rho family of small GTPases, plays a role in the biogenesis of mitochondria-associated membranes (MAMs) [22]. RAC1, a key regulator of NADPH oxidase (NOX), promotes reactive oxygen species (ROS) production via NOX activation, a critical mechanism contributing to myocardial I/R injury [23]. Although clinical myocardial I/R injury encompasses multiple pathophysiological processes following interruption and restoration of blood flow, it is challenging to fully recapitulate this cycle *in vitro* at the cellular level. Therefore, a hypoxia–reoxygenation (H/R) model in H9c2 cells was used to specifically mimic the critical "oxygen deprivation–restoration" component of I/R injury. H/R exposure in cardiomyocyte cell cultures effectively reproduces hallmark features of myocardial I/R injury, including oxidative damage, calcium dysregulation, and disturbances in mitochondrial and ER function, thus serving as a robust platform for mechanistic investigation [24,25]. In summary, this study aims to elucidate the role of ASAP3 in the regulation of myocardial I/R injury and to identify the underlying molecular mechanisms that may serve as novel therapeutic targets.

Materials and Methods

Cell Culture and Processing

The H9c2 cell line (American Type Culture Collection (ATCC), CRL-1446, Manassas, VA, USA) was cultured in high-glucose Dulbecco's Modified Eagle Medium (DMEM) supplemented with 10% fetal bovine serum (Gibco, Thermo Fisher Scientific, Waltham, MA, USA; cat. no. A5670701) and 1% antibiotics at 37 °C and 5% CO_2. To ensure the stability and reliability of the cell line, mycoplasma contamination was routinely screened using the EZ-PCR Mycoplasma Test Kit (Biological Industries, Beit HaEmek, Israel, cat. no. 20-700-20) before experimentation; all cell cultures used in this study tested negative. The identity of the H9c2 cell line was further authenticated by short tandem repeat (STR) profiling. To assess ASAP3 expression following H/R injury, H9c2 cells were cultured to 70%–80% confluence. The culture medium was then replaced with glucose- and serum-free DMEM, and the cells were incubated under hypoxic conditions (1% O_2, 94% N_2, 5% CO_2) at 37 °C for 6 hours. Subsequently, they were returned to normoxic conditions for 3, 6, 12, 18 or 24 hours before sample collection [24,26]. To evaluate the effect of different expression levels of ASAP3 on H/R injury, H9c2 cells were transfected with either the control plasmid (empty pcDNA3.1), an ASAP3 overexpression plasmid (pcDNA3.1-ASAP3, synthesized and purchased from GeneChem, Shanghai, China), or a RAC1 overexpression plasmid (pcDNA3.1-RAC1, purchased from Addgene, Watertown, MA, USA), as well as with control shRNA, ASAP3 shRNA,

and RAC1 shRNA using Lipofectamine 3000 (Thermo Fisher Scientific, Waltham, MA, USA) (**Supplementary Table 1**). The siRNA sequences targeting ASAP3 were 5′-ATAGAAAGCCCACTTTCTCCG+dTdT-3′ (sense) and 5′-GAGAAAGTGGGCTTTCTATAC+dTdT-3′ (antisense); those targeting RAC1 were 5′-TATATTCTCCAGGAAATGCAT+dTdT-3′ (sense) and 5′-GCATTTCCTGGAGAATATATC+dTdT-3′ (antisense). After 48 hours of transfection, cells were subjected to a 12-hour hypoxia-reoxygenation protocol.

Construction and Validation of RAC1 and ASAP3 Overexpression Systems

To construct the *RAC1* and *ASAP3* overexpression systems, the respective cDNAs were obtained and cloned into the pcDNA3.1 vector. The plasmid map of the pcDNA3.1(+)-RAC1 construct is provided in **Supplementary Fig. 1**. The *RAC1* and *ASAP3* gene fragments were amplified and digested with EcoRI and XhoI, followed by ligation into the multiple cloning site of the pcDNA3.1 vector to ensure proper orientation and expression under the vector's promoter. The recombinant plasmids were verified by restriction enzyme digestion and sequencing to confirm successful insertion.

Subsequently, the plasmids (pcDNA3.1-*RAC1* and pcDNA3.1-*ASAP3*) were transfected into H9c2 cells using Lipofectamine 3000. Transfection efficiency was assessed by quantitative real-time polymerase chain reaction (qRT-PCR), which demonstrated significant upregulation of *RAC1* and *ASAP3* mRNA in the overexpression groups compared to controls. Protein levels of RAC1 and ASAP3 were validated by Western blot. To investigate the potential interaction between ASAP3 and RAC1, co-immunoprecipitation (Co-IP) assays were conducted. Cell lysates were incubated with anti-ASAP3 antibody, and immunoprecipitated complexes were analyzed by Western blot using anti-RAC1 antibody. The detection of RAC1 in ASAP3 immunoprecipitates confirmed a direct interaction between the two proteins. These experiments demonstrated the successful construction of pcDNA3.1-*RAC1* and pcDNA3.1-*ASAP3* overexpression systems and validated both their expression and the interaction of their protein products in H9c2 cells.

qRT-PCR

Total RNA was extracted from cells homogenized in 1 mL TRIzol® reagent. RNA concentration and purity were determined using a NanoDrop ND-2000 spectrophotometer (Thermo Fisher Scientific, Waltham, MA, USA), with purity assessed by the A260/A280 ratio. cDNA synthesis was performed using SuperScript IV Reverse Transcriptase (K1612, Thermo Fisher Scientific, Waltham, MA, USA) according to the manufacturer's instructions. The resulting cDNA was diluted 1:5 with nuclease-free water for subsequent quantitative PCR. Quantitative PCR was performed using PowerUp SYBR Green Master Mix (A25742, Thermo Fisher Scientific, Waltham, MA, USA) on a QuantStudio 7 Real-Time PCR System (Thermo Fisher Scientific, Waltham, MA, USA). Relative gene expression was calculated using the $2^{-\Delta\Delta Ct}$ method, with glyceraldehyde-3-phosphate dehydrogenase (GAPDH) used as the endogenous control. Expression levels of ASAP3 and RAC1 in the treatment group were normalized to controls. The specific primer sequences used are listed in Table 1.

Table 1. Primers for qRT-PCR.

Gene name	Sequences (5′ to 3′)
ASAP3	F: CGGAAGAACTCAGGATGTGGCT
	R: AGGCAGCCATACTTGACTCCAC
RAC1	F: GACTCCCATCACCTATCCGC
	R: CTCGGATCGCTTCGTCAAAC
GAPDH	F: GTCTCCTCTGACTTCAACAGCG
	R: ACCACCCTGTTGCTGTAGCCAA

qRT-PCR, quantitative real-time polymerase chain reaction; *ASAP3*, adenosine diphosphate-ribosylation factor GTPase-activating protein (ArfGAP) with homology 3 (SH3) domain, ankyrin repeat, and pleckstrin homology (PH) domain-containing protein 3; *RAC1*, ras-related C3 botulinum toxin substrate 1; *GAPDH*, glyceraldehyde-3-phosphate dehydrogenase.

Cell Viability Assays

H9c2 cells (1×10^4/well) were seeded into 96-well plates and incubated for 24 hours, followed by transfection and hypoxia-reoxygenation treatment. Thirty minutes before the end of treatment, 10 µL of Cell Counting Kit-8 reagent (CCK-8; Beyotime, Shanghai, China; cat. no. C0038) was added to each well. The plates were further incubated for 4 hours at 37 °C in a CO_2 incubator until a visible color change occurred. Optical density (OD) values were measured at 450 nm using a Multiskan Sky microplate reader (Thermo Fisher Scientific, Waltham, MA, USA). Cell viability was calculated as a percentage relative to the control group, which was defined as 100%.

Apoptosis Assays

H9c2 cells (1×10^6/well) were seeded into 6-well plates and incubated for 24 hours, followed by transfection and hypoxia-reoxygenation treatment. After treatment, the medium was discarded, and cells were trypsinized and collected by centrifugation at 1000 rpm for 5 minutes. Cells were washed twice with phosphate-buffered saline (PBS) to remove residual media. Using the Annexin V-fluorescein isothiocyanate (FITC)/propidium iodide (PI) apoptosis detection kit (BD Biosciences, Franklin Lakes, NJ, USA; cat. no. 556547), cells were resuspended at 1×10^6 cells/mL in binding buffer and incubated with 5 µL Annexin V-FITC

and 10 µL PI for 30 minutes at room temperature in the dark. Apoptotic cells were analyzed by flow cytometry (FACSCanto II) with fluorescence detection at 530 nm and 610 nm emission wavelengths.

Immunofluorescence Detection

After treatment, H9c2 cells (1×10^6 cells/well) were plated into 6-well plates, rinsed twice with PBS, and incubated with 1 µM Fluo-4 AM (F14201, Thermo Fisher Scientific, Waltham, MA, USA) at 37 °C for 30 min. After washing with PBS, fluorescence images were obtained using a Leica DMi8 microscope (excitation 494 nm, emission 516 nm). In parallel, JC-1 dye (2 µM, T3168) was used to assess mitochondrial membrane potential, with excitation at 490 nm and emission at 525 nm.

Assessment of Cellular ATP Levels and Mitochondrial ROS Production

Intracellular adenosine triphosphate (ATP) levels were measured using a luciferase-based ATP assay kit (S0026, Beyotime, China) according to the manufacturer's guidelines. Cells were lysed on ice for 5 min and centrifuged at 12,000 ×g for 5 min at 4 °C. Equal volumes of ATP detection working solution and sample or standard were mixed in a 96-well plate. Luminescence was recorded within 5 minutes using a microplate reader (model Synergy2, BioTek Instruments, Winooski, VT, USA). ATP concentrations were normalized to total protein and expressed as relative ATP levels. Mitochondrial ROS production was assessed in parallel using the MitoSOX Red mitochondrial superoxide indicator (S0061S, Beyotime, China). Cells were incubated with 5 µM MitoSOX Red in serum-free medium at 37 °C for 30 min. After rinsing with PBS, fluorescence was measured (excitation 561 nm, emission 585 nm) using the same microplate reader. ROS levels were normalized to total protein and reported as fold change relative to the control.

Western Blot

PBS-washed H9c2 cells were lysed in radioimmunoprecipitation assay (RIPA) buffer and incubated on ice for 15 minutes. Lysates were centrifuged at 12,000 rpm for 10 minutes, and protein concentrations were determined using the bicinchoninic acid (BCA) kit (23225, Thermo Fisher Scientific, Waltham, MA, USA). Equal amounts of protein (30 µg per sample) were mixed with 5 × sample buffer (P0015, Beyotime, China), denatured, and loaded onto a 10% sodium dodecyl sulfate–polyacrylamide gel electrophoresis (SDS-PAGE) gel. Proteins were then transferred onto polyvinylidene difluoride (PVDF) membranes at 100 V for 1 hour. After blocking with 5% non-fat milk, membranes were incubated overnight at 4 °C with the following primary antibodies: ASAP3 (differentiation-enhancing factor-like 1 (DDEFL1), 1:1000, GTX120116, GeneTex, Irvine, CA, USA), RAC1 (1:1000, #4651, CST, Danvers, MA, USA), inositol 1,4,5-trisphosphate receptor (IP3R, 1:1000, ab264281, Abcam, Cambridge, UK), Mitofusin-2 (MFN2, 1:1000, #9482, CST, USA), sigma-1 receptor (Sig-1r, 1:1000, ab307548, Abcam, UK), C/EBP homologous protein (CHOP, 1:1000, 2895, CST, USA), PKR-like endoplasmic reticulum kinase (PERK, 1:1000, 3192, CST, USA), phosphorylated PERK (p-PERK, 1:1000, 3179, CST, USA), and β-actin (1:1000, 4970, CST, USA). After washing, membranes were incubated at room temperature with horseradish peroxidase (HRP)-conjugated secondary antibodies: goat anti-mouse immunoglobulin G (IgG) (H+L, 1:5000, A0350, Beyotime, China) and goat anti-rabbit IgG (H+L, 1:5000, A0352, Beyotime, China). Bands were visualized using enhanced chemiluminescence (ECL, 32106, Thermo Fisher Scientific, Waltham, MA, USA), and images were captured with a ChemiDoc MP imaging system (Bio-Rad Laboratories, Hercules, CA, USA). Densitometric analysis was performed using ImageJ software (version 1.53k, National Institutes of Health, Bethesda, MD, USA), and protein expression levels were normalized to β-actin. For detection of RAC1-GTP (GTP: guanosine triphosphate), RAC1-GTP was enriched from cell lysates using a RAC1-GTP pull-down kit (BK036, Cytoskeleton, Denver, CO, USA) prior to electrophoresis, followed by analysis with a RAC1 antibody (1:1000, #2465, CST, USA) to assess its expression level.

Co-Immunoprecipitation (Co-IP) Assay

Co-immunoprecipitation was performed using the Pierce™ Co-IP Kit (Thermo Fisher Scientific, Waltham, MA, USA) to investigate whether ASAP3 interacts with RAC1. H9c2 cells were lysed in IP lysis buffer containing protease inhibitors. Cell lysates (500 µg) were incubated overnight at 4 °C with an anti-ASAP3 antibody (1:1000, 14099-1-AP, Proteintech, Wuhan, China), followed by incubation with Protein A/G agarose beads for 2 hours. After extensive washing, the immunoprecipitates were denatured in sample SDS buffer and subjected to Western blot using an anti-RAC1 antibody (1:500, 24072-1-AP, Proteintech, China) and goat anti-rabbit IgG (H+L, 1:5000, A0352, Beyotime, China). Rabbit IgG was used as a negative control.

Statistical Analysis

Data were analyzed using GraphPad Prism 8 (GraphPad Software, San Diego, CA, USA). One-way analysis of variance (ANOVA) followed by Tukey's post hoc test was used for multiple group comparisons. Data are presented as mean ± standard deviation (SD). Differences were considered statistically significant at $p < 0.05$. All experiments were independently repeated at least three times, with specific sample sizes (n) indicated in the figure legends. Graphs were generated using GraphPad Prism 8.

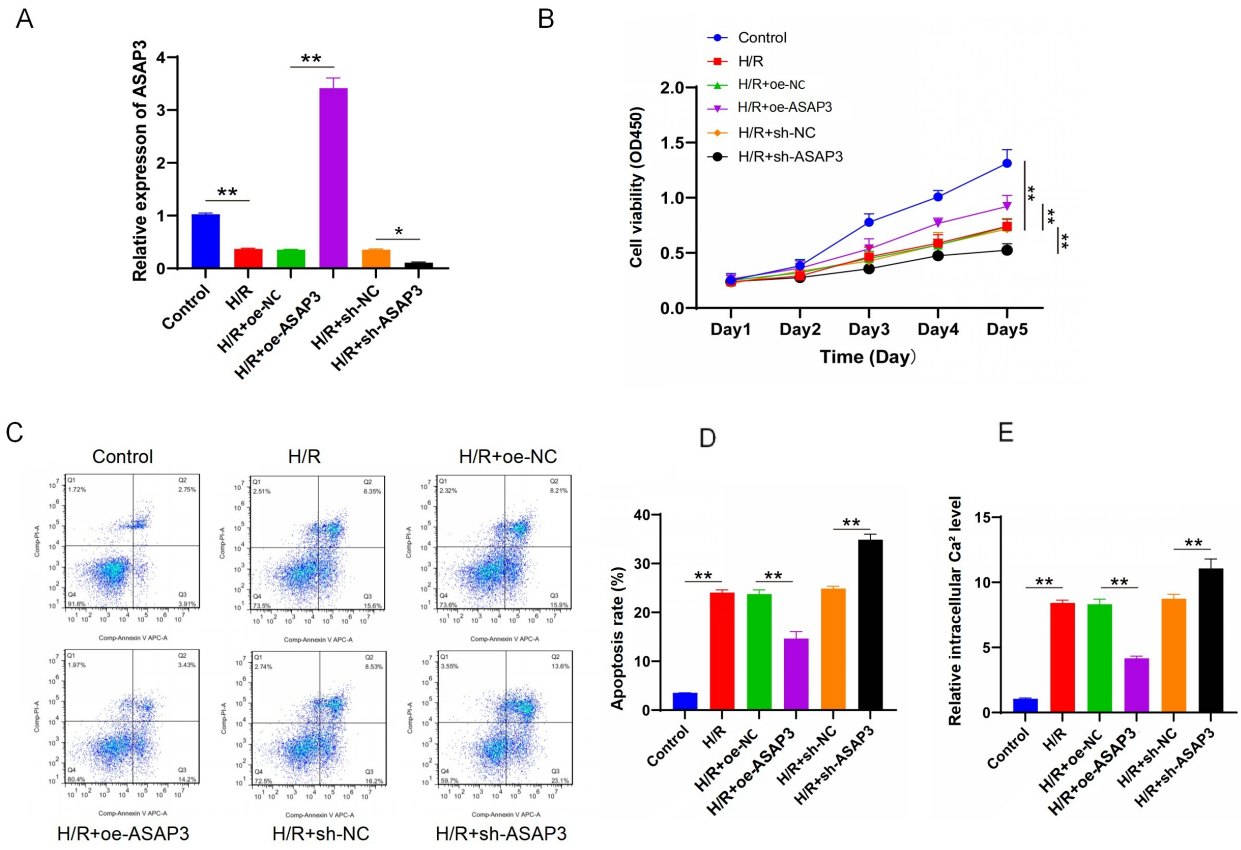

Fig. 1. ASAP3 overexpression promotes the viability of H9c2 cells following H/R and inhibits apoptosis and intracellular Ca^{2+} accumulation. (A) ASAP3 mRNA expression in H9c2 cells from the control group and the following treatment groups: H/R, H/R + oe-NC, H/R + oe-ASAP3, H/R + sh-NC, H/R + sh-ASAP3, measured by qRT-PCR. (B) Cell viability was assessed by CCK-8 assay. (C,D) Flow cytometry was used to quantify apoptosis in H9c2 cells. (E) Intracellular Ca^{2+} levels were evaluated by immunofluorescence. * $p < 0.05$, ** $p < 0.01$ (n = 3). H/R, Hypoxia-reperfusion; qRT-PCR, quantitative real-time PCR; oe-NC, negative-control overexpression vector; oe-ASAP3, ASAP3 overexpression; sh-NC, negative-control shRNA; sh-ASAP3, ASAP3 knockdown; CCK-8, Cell Counting Kit-8.

Results

ASAP3 Overexpression Promotes H/R-Induced Viability of H9c2 Cells and Inhibits Apoptosis and Ca^{2+} Accumulation

ASAP3 transfection efficiency was confirmed by assessing mRNA and protein levels using qRT-PCR and Western blot. Compared with the oe-NC (negative control overexpression) group, ASAP3 expression was significantly upregulated in the oe-ASAP3 group. Conversely, compared with the sh-NC (negative control knockdown) group, ASAP3 expression was notably downregulated in the sh-ASAP3 group ($p < 0.01$; **Supplementary Fig. 2A**). Under hypoxia-reoxygenation (H/R) conditions, ASAP3 mRNA levels in the H/R group were significantly lower than those in the control group ($p < 0.01$; Fig. 1A). Functionally, relative to H/R + oe-NC, the H/R + oe-ASAP3 group exhibited significantly increased cell viability, decreased apoptosis, and reduced intracellular Ca^{2+} accumulation (all $p < 0.01$; Fig. 1B–E). In contrast, the H/R + sh-ASAP3 group showed opposite effects compared to the H/R + sh-NC group (all $p < 0.01$; Fig. 1B–E). These findings suggest that ASAP3 plays a critical role in regulating endoplasmic reticulum-mitochondrial dynamics during H/R.

ASAP3 Overexpression Ameliorates H/R-Induced MAM Dysfunction in H9c2 Cells

In H9c2 cells exposed to H/R, levels of RAC1 and RAC1-GTP increased significantly compared to the control group ($p < 0.01$; Fig. 2A). ASAP3 overexpression reversed these increases (compared to H/R + oe-NC), while ASAP3 knockdown further elevated them (compared to H/R + sh-NC). Similarly, H/R significantly upregulated ER stress markers, including IP3R, CHOP, and the p-PERK/PERK ratio, while downregulating MFN2 and Sig-1R (all $p < 0.01$; Fig. 2B). ASAP3 overexpression mitigated these changes, whereas ASAP3 knockdown exacerbated them. Collectively, these data indicate that ASAP3 overexpression alleviates H/R-induced MAM dysfunction.

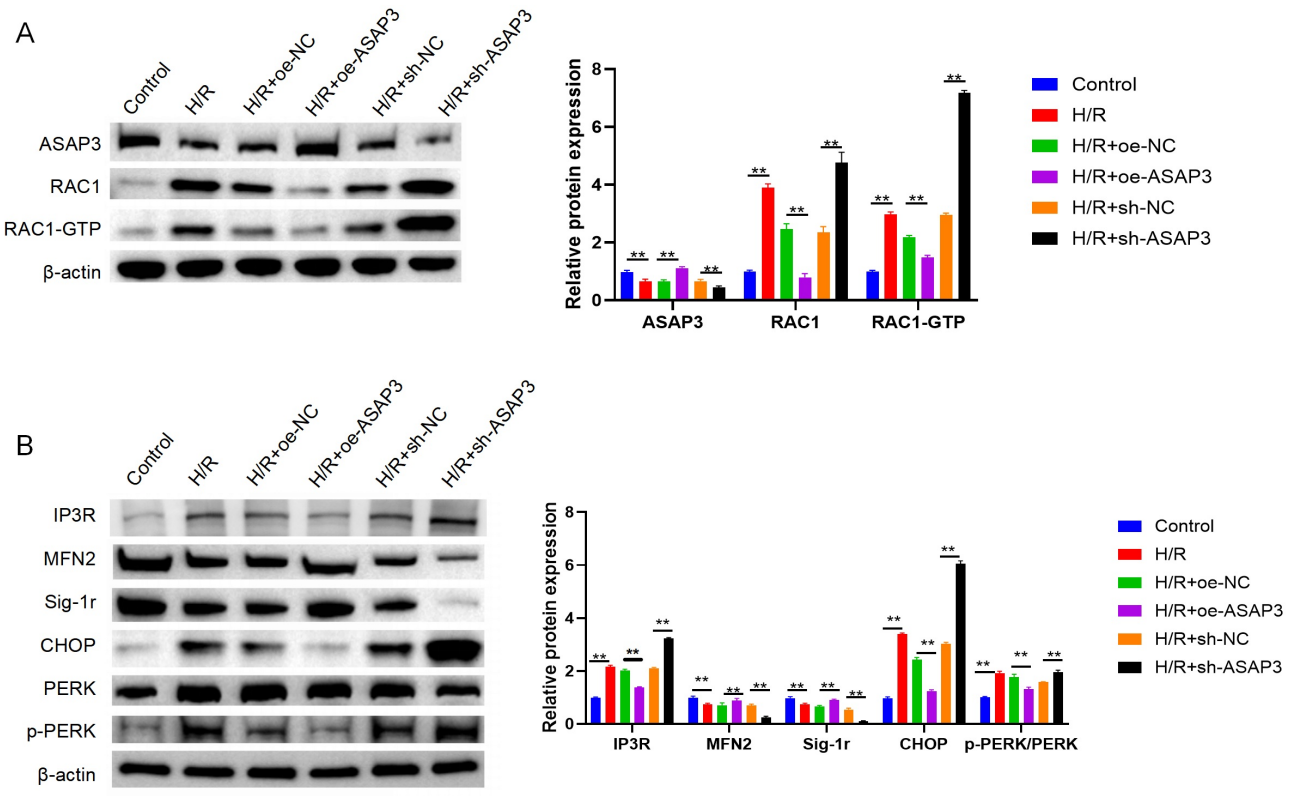

Fig. 2. ASAP3 overexpression ameliorates H/R-caused MAM dysfunction in H9c2 cells. (A) Western blot was conducted to observe the protein expression levels of RAC1 and RAC1-GTP in H9c2 cells in the control, H/R, H/R + oe-NC, H/R + oe-ASAP3, H/R + sh-NC, and H/R + sh-ASAP3 groups. (B) Western blot of the protein levels of IP3R, MFN2, Sig-1r, CHOP, PERK, and p-PERK in H9c2 cells in the control, H/R, H/R + oe-NC, H/R + oe-ASAP3, H/R + sh-NC, and H/R + sh-ASAP3 groups. ** $p < 0.01$ (n = 3). H/R, Hypoxia-reperfusion; MAM, mitochondria-associated endoplasmic reticulum membrane; RAC1, Ras-related C3 botulinum toxin substrate 1; IP3R, inositol 1,4,5-trisphosphate receptor; MFN2, mitofusin-2; Sig-1R, sigma-1 receptor; CHOP, C/EBP homologous protein; PERK, PKR-like endoplasmic reticulum kinase; p-PERK, phosphorylated PERK; oe-NC, negative-control overexpression vector; oe-ASAP3, ASAP3 overexpression; sh-NC, negative-control shRNA; sh-ASAP3, ASAP3 knockdown.

Overexpression of ASAP3 Alleviates Mitochondrial Injury Induced by H/R in H9c2 Cells

Additionally, a notable elevation in mitochondrial ROS levels was observed in H9c2 cells exposed to H/R, as well as in the H/R + sh-ASAP3 group, which was accompanied by a marked decrease in both JC-1 and ATP levels. Conversely, overexpression of ASAP3 under H/R conditions significantly suppressed mitochondrial ROS and led to increased JC-1 and ATP levels ($p < 0.05$, Fig. 3A–D), underscoring the protective role of ASAP3 against mitochondrial dysfunction.

RAC1 Reverses the Regulatory Effects of ASAP3 Overexpression on Cell Viability, Apoptosis, and Intracellular Ca^{2+} Accumulation Under H/R Conditions in H9c2 Cells

qRT-PCR and Western blot analyses showed that RAC1 mRNA and protein levels were significantly elevated in the oe-RAC1 group compared to the oe-NC group ($p < 0.01$, **Supplementary Fig. 2B**) indicating successful overexpression. Given that ASAP3 is downregulated under H/R conditions and its overexpression alleviates cell injury, we further explored the interaction and functional roles of ASAP3 and RAC1 during H/R. Since ASAP3 regulates RAC1 expression, CCK-8, Annexin V-FITC/PI staining, and Fluo-4 AM assays were performed to evaluate cell viability, apoptosis, and intracellular Ca^{2+} levels, respectively. The H/R + oe-ASAP3 + RAC1 group displayed significantly lower viability, higher apoptosis rates, and increased intracellular Ca^{2+} levels compared to the H/R + oe-ASAP3 group ($p < 0.01$, Fig. 4A–C). Conversely, in comparison to the H/R + oe-RAC1 group, the H/R + oe-ASAP3 + RAC1 group showed improved cell viability and reduced apoptosis and Ca^{2+} levels ($p < 0.01$). Furthermore, to assess a potential interaction between ASAP3 and RAC1, a Co-IP assay was performed. Using an ASAP3 antibody for immunoprecipitation from H9c2 cell lysates, subsequent Western blot analysis detected RAC1 in the ASAP3 immunoprecipitates, indicating a direct physical interaction (Fig. 4D). Collectively, these findings suggest that RAC1

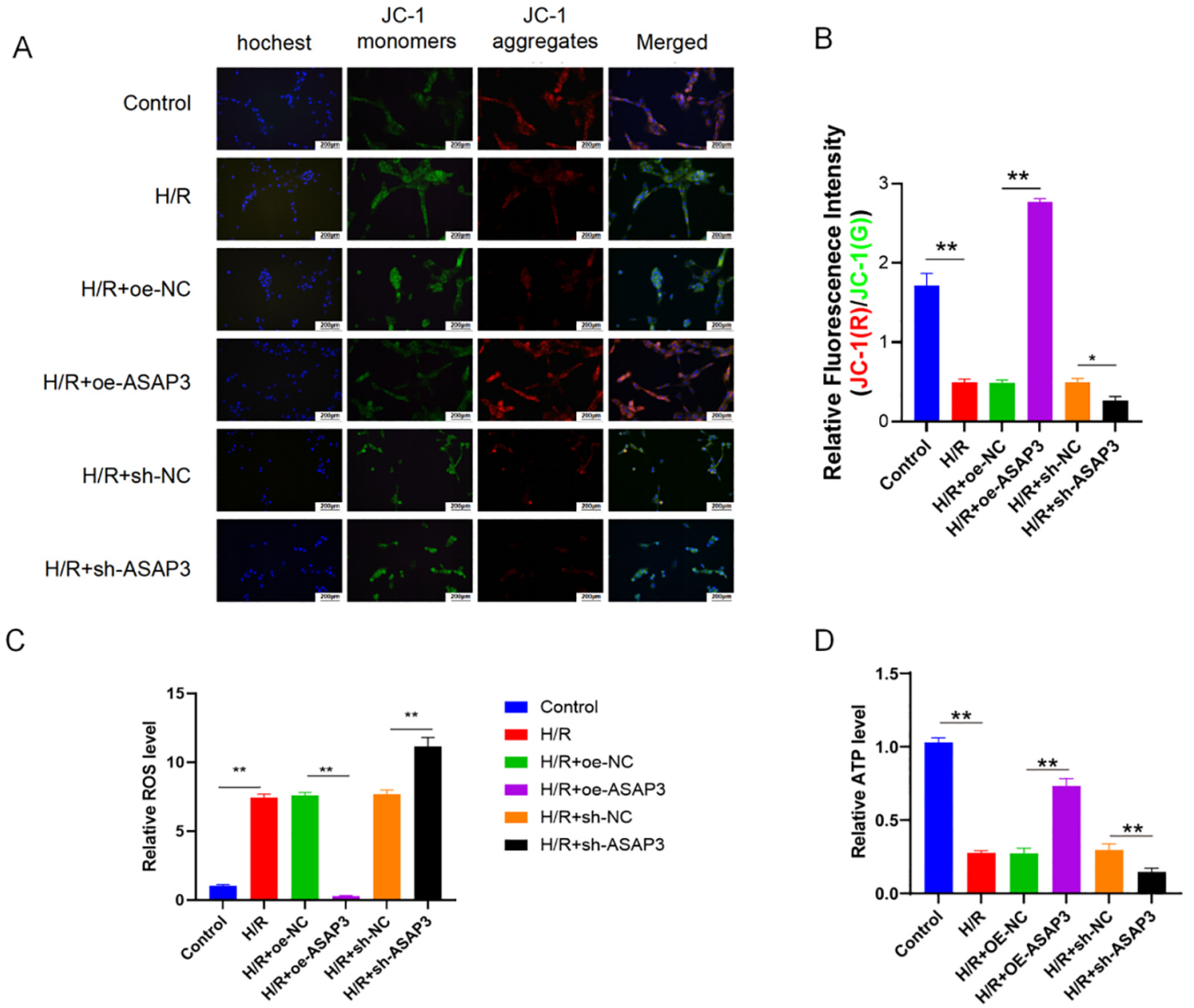

Fig. 3. Overexpression of ASAP3 attenuates mitochondrial damage caused by H/R in H9c2 cells. (A–C) Kits were used to detect the levels of mitochondrial JC-1 (A,B), ROS (C), and ATP (D) in H9c2 cells of the control, H/R, H/R + oe-NC, H/R + oe-ASAP3, H/R + sh-NC, and H/R + sh-ASAP3 groups. *$p < 0.05$, ** $p < 0.01$. Scale bar = 200 µm (n = 3). H/R, hypoxia-reperfusion; JC-1, 5,5′,6,6′-tetrachloro-1,1′,3,3′-tetraethylbenzimidazolylcarbocyanine iodide; ROS, reactive oxygen species; ATP, adenosine triphosphate; oe-NC, negative-control overexpression vector; oe-ASAP3, ASAP3 overexpression; sh-NC, negative-control shRNA; sh-ASAP3, ASAP3 knockdown.

can antagonize the protective effects conferred by ASAP3 overexpression in H9c2 cells subjected to H/R injury, potentially through a direct binding mechanism.

RAC1 Alleviates the Impact of ASAP3 Overexpression on H/R-Induced Mitochondrial Damage in H9c2 Cells

Assessment of mitochondrial ROS indicated a notable increase in the H/R + oe-ASAP3 + RAC1 group compared to the H/R + oe-ASAP3 group, accompanied by a substantial decrease in JC-1 and ATP levels. Conversely, when compared to the H/R + oe-RAC1 group, H9c2 cells in the H/R + oe-ASAP3 + RAC1 group demonstrated a significant reduction in mitochondrial ROS levels, while JC-1 and ATP levels were significantly elevated ($p < 0.01$, Fig. 5A–D). These findings suggest that RAC1 mitigates the effects of ASAP3 overexpression on mitochondrial injury following H/R-induced stress.

RAC1 Compromises ASAP3-Mediated Protection Against H/R-Induced MAM Dysfunction in H9c2 Cells

Compared to the H/R + oe-RAC1 group, the H/R + oe-ASAP3 + RAC1 group exhibited significantly decreased levels of total RAC1 and RAC1-GTP ($p < 0.01$, Fig. 6A). Moreover, this group displayed higher IP3R and CHOP levels, an increased p-PERK/PERK ratio, and reduced levels of MFN2 and Sig-1r relative to the H/R + oe-ASAP3

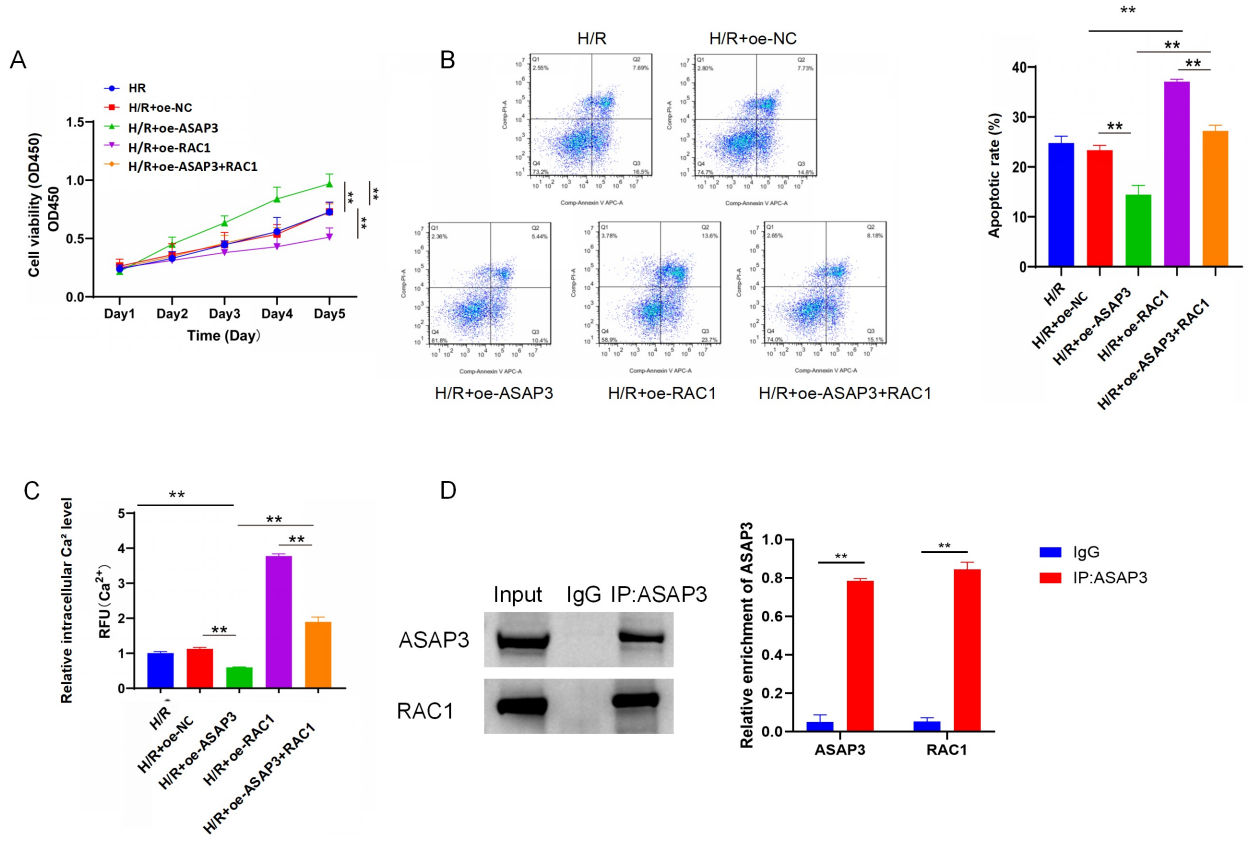

Fig. 4. RAC1 alleviates the impact of ASAP3 overexpression on H/R-induced H9c2 cell viability, apoptosis, and Ca^{2+} accumulation. (A) Viability of H9c2 cells under various conditions (H/R, H/R + oe-NC, H/R + oe-ASAP3, H/R + oe-RAC1, H/R + oe-ASAP3 + RAC1) was measured using CCK-8 assay. (B) Apoptosis in H9c2 cells was evaluated using flow cytometry. (C) Ca^{2+} in H9c2 cells was measured using immunofluorescence. (D) Co-IP assays demonstrated the interaction with ASAP3 and RAC1 in H9c2 cells. ** $p < 0.01$ (n = 3). H/R, hypoxia-reperfusion; CCK-8, Cell Counting Kit-8; Co-IP, co-immunoprecipitation; ASAP3, ArfGAP with SH3 domain, ankyrin repeat and PH domain 3; RAC1, Ras-related C3 botulinum toxin substrate 1; oe-NC, negative-control overexpression vector; oe-ASAP3, ASAP3 overexpression; sh-NC, negative-control shRNA; sh-ASAP3, ASAP3 knockdown.

group, as determined by Western blot analysis ($p < 0.01$, Fig. 6B). These findings indicate enhanced ER stress and further suggest that RAC1 impairs the protective effects of ASAP3 in maintaining MAM homeostasis following H/R injury (Fig. 7).

Discussion

I/R injury involves multiple complex cellular and molecular events, including oxidative stress, calcium overload, apoptosis, inflammation, and mitochondrial dysfunction [25]. Understanding these pathways is crucial for identifying molecular targets and developing cardioprotective drugs. Our results indicate that ASAP3 may confer protection against I/R injury and could serve as a potential target for future therapeutic strategies.

ASAP3, previously studied mainly in cancer cell migration and invasion, regulates cytoskeletal dynamics, membrane trafficking, and actin remodeling as a GTPase. Originally named DDEFL1, it shares substrates and domain architecture with other members of the ASAP family [27,28]. In this study, we observed a significant reduction in ASAP3 expression in H9c2 cells following H/R. Overexpression of ASAP3 notably enhanced cell viability and reduced apoptosis.

Further experiments revealed that ASAP3 overexpression improved H9c2 cell tolerance to H/R injury. Previous studies have shown that ischemia impairs the Na^+/K^+ pump, leading to intracellular sodium accumulation. Consequently, the Na^+/Ca^{2+} exchanger operates in reverse mode, driving calcium overload, which is exacerbated upon reperfusion [29,30]. This calcium overload disrupts mitochondrial membrane potential, reduces ATP synthesis, and activates destructive enzymatic cascades, ultimately inducing apoptosis or necrosis [31,32]. In our study, ASAP3-overexpressing cells showed significantly reduced Ca^{2+} accumulation, suggesting that ASAP3 may help preserve mitochondrial and membrane integrity.

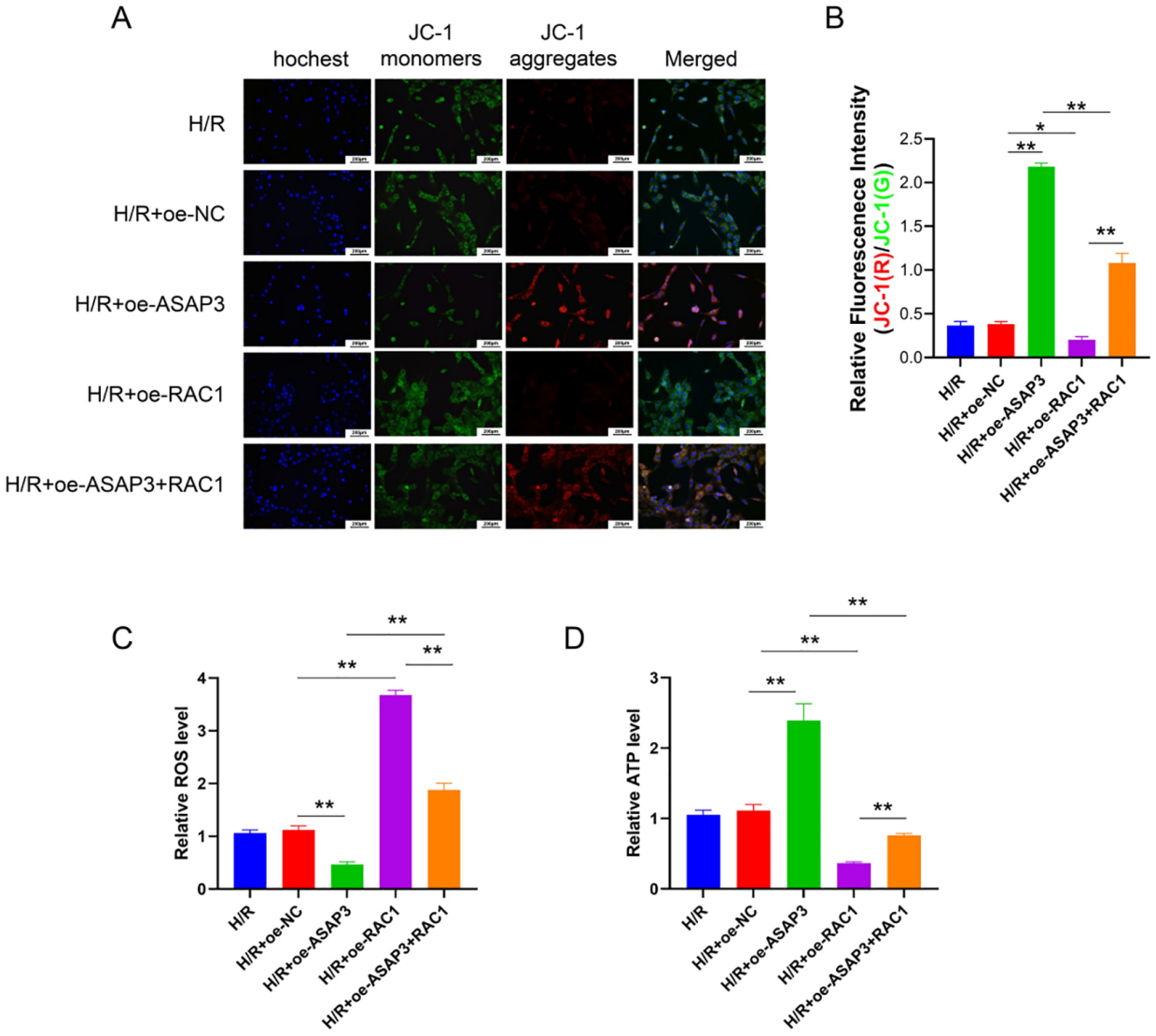

Fig. 5. RAC1 alleviates the influence of ASAP3 overexpression on H/R-induced mitochondrial damage in H9c2 cells. (A–C) Kits were used to detect the levels of mitochondrial JC-1 (A,B), ROS (C), and ATP (D) in H9c2 cells from the H/R, H/R + oe-NC, H/R + oe-ASAP3, H/R + oe-RAC1, and H/R + oe-ASAP3 + RAC1 groups. *$p < 0.05$, ** $p < 0.01$ (n = 3). Scale bar = 200 µm. H/R, hypoxia-reperfusion; JC-1, 5,5′,6,6′-tetrachloro-1,1′,3,3′-tetraethylbenzimidazolylcarbocyanine iodide; ROS, reactive oxygen species; ATP, adenosine triphosphate; ASAP3, ArfGAP with SH3 domain, ankyrin repeat and PH domain 3; RAC1, Ras-related C3 botulinum toxin substrate 1; oe-NC, negative-control overexpression vector; oe-ASAP3, ASAP3 overexpression; sh-NC, negative-control shRNA; sh-ASAP3, ASAP3 knockdown.

MAMs, which physically connect mitochondria and the ER, play a central role in Ca^{2+} transfer, lipid metabolism, and mitochondrial dynamics [33–35]. ASAP3, as a known regulator of Arf6, may influence MAM structure by modulating cytoskeletal elements involved in membrane interactions [36]. These findings suggest that ASAP3 preserves MAM function during H/R by reducing ROS, restoring mitochondrial membrane potential and ATP levels, and mitigating ER stress.

RAC1, a small GTPase of the Rho family, has been implicated in myocardial injury by regulating oxidative stress, apoptosis, inflammation, and cytoskeletal remodeling [37,38]. RAC1 activates NADPH oxidase via p67phox, thereby elevating ROS production [39], and promotes apoptosis through the JNK and p38 MAPK signaling pathways [40,41]. Additionally, RAC1 enhances intracellular Ca^{2+} levels by activating L-type calcium channels and inducing ER calcium release [42]. In our study, ASAP3 and RAC1 exhibited opposing effects in cells subjected to H/R stress. Interestingly, prior cancer research has reported a positive correlation between ASAP3 and Rho proteins [43], highlighting the complexity and context-dependent nature of their interaction.

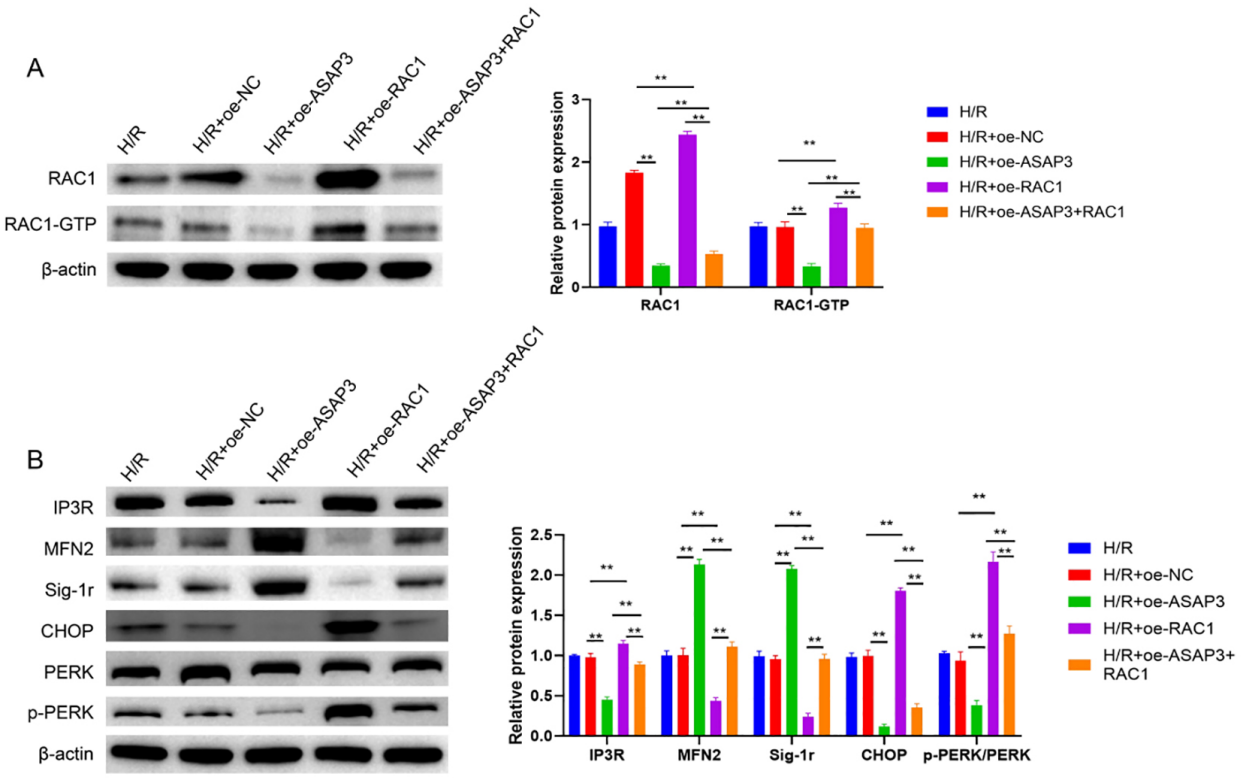

Fig. 6. The regulatory effect of ASAP3 on H/R-induced MAM disruption is attenuated by RAC1 in H9c2 cells. (A) Western blot detection of RAC1 and RAC1-GTP in H9c2 cells in the H/R, H/R + oe-NC, H/R + oe-ASAP3, H/R + oe-RAC1, and H/R + oe-ASAP3 + RAC1 groups. (B) Western blot detection of IP3R, MFN2, Sig-1r, CHOP, PERK, and p-PERK in H9c2 cells in the control, H/R, H/R + oe-NC, H/R + oe-ASAP3, H/R + sh-NC, and H/R + sh-ASAP3 groups. ** $p < 0.01$ (n = 3). H/R, hypoxia-reperfusion; MAM, mitochondria-associated endoplasmic reticulum membrane; ASAP3, ArfGAP with SH3 domain, ankyrin repeat and PH domain 3; oe-NC, negative-control overexpression vector; oe-ASAP3, ASAP3 overexpression; sh-NC, negative-control shRNA; sh-ASAP3, ASAP3 knockdown.

To distinguish between active and total RAC1 protein levels, we analyzed RAC1-GTP alongside total RAC1. RAC1-GTP represents the GTP-bound, active form that mediates downstream signaling, while total RAC1 reflects both active and inactive forms. We observed that RAC1 and RAC1-GTP showed similar expression patterns across groups, and the RAC1-GTP to total RAC1 ratio remained relatively constant. This suggests that changes in total RAC1 levels corresponded to parallel changes in activation status. Presenting total and active forms separately is consistent with previous studies and helps avoid redundancy while improving data interpretability. In contrast, for PERK, we directly quantified and presented the p-PERK/PERK ratio, and phosphorylation significantly changed independently of total PERK levels.

ASAP3 appears to function as a protective factor in myocardial ischemia-reperfusion injury, whereas its known functions in tumor cells are primarily associated with migration and invasion. This apparent divergence suggests the existence of cell-type-specific regulatory mechanisms. Such differences may arise from variations in protein interaction networks, subcellular localization, or signaling environments of ASAP3 in cardiomyocytes compared to cancer cells. Future studies using single-cell transcriptomics or proteomics may uncover the unique regulatory pathways of ASAP3 in cardiac tissue.

Although our current findings highlight the significance of ASAP3 at the cellular level, clinical evidence linking its expression to cardiovascular outcomes remains limited. Incorporating analyses of patient tissue samples or leveraging public datasets to correlate ASAP3 expression with clinical parameters, such as infarct size, cardiac functional recovery, and long-term survival, would further validate its potential as a prognostic marker.

In addition, the therapeutic potential of ASAP3 warrants additional investigation. Its ArfGAP domain, which functions as a molecular switch regulator, represents a promising pharmacological target. Structure-based drug screening for small-molecule inhibitors of ASAP3 could be a viable therapeutic strategy. Furthermore, combining ASAP3-targeted modulation with existing cardioprotective agents, such as antioxidants, mitochondrial protectants, or calcium channel blockers, may enhance treatment efficacy against I/R injury.

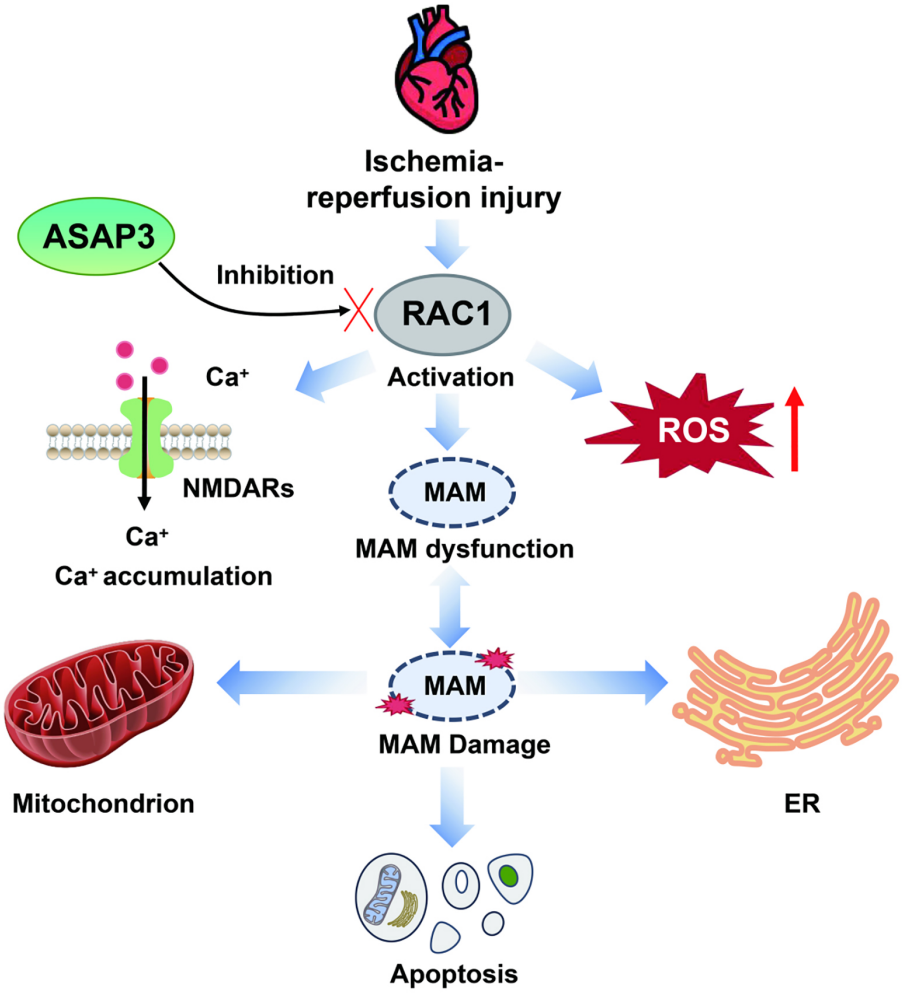

Fig. 7. Mechanism by which ASAP3 protects against myocardial ischemia–reperfusion injury. I/R injury activates RAC1, leading to excessive reactive oxygen species (ROS) production, Ca^{2+} overload (mediated by NMDARs), and dysfunction of mitochondrial-associated endoplasmic reticulum membranes (MAMs). This cascade contributes to MAM structural damage and apoptosis. ASAP3 overexpression suppresses RAC1 activation, thereby preserving MAM integrity, reducing mitochondrial injury, and attenuating cardiomyocyte cell death. The red upward arrow indicates increased ROS production, and the red cross mark denotes the inhibitory effect of ASAP3 on RAC1 activation.

While our research highlights the involvement of ASAP3 in I/R injury, it remains unclear whether a definitive mechanistic link exists between ASAP3 and RAC1. Additionally, we did not investigate the function of ASAP3 *in vivo*. In summary, comprehensive studies are necessary to elucidate the detailed mechanisms of ASAP3 action to be validated as a potential therapeutic target.

Conclusions

In conclusion, ASAP3 levels were significantly reduced in H9c2 cells subjected to hypoxia-reoxygenation, which was associated with reduced cell viability and elevated apoptosis. Furthermore, ASAP3 was found to support the maintenance of physiological MAM function, as well as mitochondrial and endoplasmic reticulum integrity, in H9c2 cells following reoxygenation after hypoxic stress by inhibiting RAC1 activation. This regulatory effect helps maintain cell viability and modulate apoptosis. Our study highlights ASAP3 as a potential molecular target for the treatment of I/R-related damage.

Availability of Data and Materials

The data used to support the findings of this study are available from the corresponding authors upon request.

Author Contributions

ZY contributed to conceptualization, data curation, formal analysis, and visualization, and drafted the original manuscript. YT participated in data curation and investigation, and assisted in manuscript review and editing. HY was involved in investigation, validation, and literature search.

YW contributed to investigation and visualization, while XL participated in investigation and validation. LF was responsible for methodology and assisted in manuscript review and editing. WX contributed to validation and visualization. YL participated in conceptualization and methodology, and YH contributed to conceptualization and supervision. All authors contributed to the drafting and critical revision of the manuscript, have read and approved the final version, and agree to be accountable for all aspects of the work.

Ethics Approval and Consent to Participate

Not applicable.

Acknowledgment

Not applicable.

Funding

This study was supported by the Regional Fund Project of the National Natural Science Foundation (grant no. 82060062); the Joint special fund of Applied Fundamental Research of Kunming Medical University granted by Science and Technology Office of Yunnan (grant nos. 202001AY070001-167 and 202101AY070001-200); the Training plan for medical leading talents of Yunnan Health Commission (grant no. L-2017007); the 14th Five-Year Plan key discipline construction project of Kunming Medical University.

Conflict of Interest

The authors declare no conflict of interest.

Supplementary Material

Supplementary material associated with this article can be found, in the online version, at https://doi.org/10.24976/Discov.Med.202537200.172.

References

[1] Bouchard K, Dans M, Higdon G, Quinlan B, Tulloch H. Caregiver Distress and Coronary Artery Disease: Prevalence, Risk, Outcomes, and Management. Current Cardiology Reports. 2022; 24: 2081–2096. https://doi.org/10.1007/s11886-022-01810-5.

[2] Rozemeijer S, Hemilä H, van Baaren M, de Man AME. Vitamin C may reduce troponin and CKMB levels after PCI and CABG: a meta-analysis. BMC Cardiovascular Disorders. 2023; 23: 475. https://doi.org/10.1186/s12872-023-03459-6.

[3] Algoet M, Janssens S, Himmelreich U, Gsell W, Pusovnik M, Van den Eynde J, *et al*. Myocardial ischemia-reperfusion injury and the influence of inflammation. Trends in Cardiovascular Medicine. 2023; 33: 357–366. https://doi.org/10.1016/j.tcm.2022.02.005.

[4] Xiang Q, Yi X, Zhu XH, Wei X, Jiang DS. Regulated cell death in myocardial ischemia-reperfusion injury. Trends in Endocrinology and Metabolism: TEM. 2024; 35: 219–234. https://doi.org/10.1016/j.tem.2023.10.010.

[5] Wang K, Zhu Q, Liu W, Wang L, Li X, Zhao C, *et al*. Mitochondrial apoptosis in response to cardiac ischemia-reperfusion injury. Journal of Translational Medicine. 2025; 23: 125. https://doi.org/10.1186/s12967-025-06136-8.

[6] Fang L, Yu Z, Qian X, Fang H, Wang Y. LDHA exacerbates myocardial ischemia-reperfusion injury through inducing NLRP3 lactylation. BMC Cardiovascular Disorders. 2024; 24: 651. https://doi.org/10.1186/s12872-024-04251-w.

[7] Ramachandra CJA, Hernandez-Resendiz S, Crespo-Avilan GE, Lin YH, Hausenloy DJ. Mitochondria in acute myocardial infarction and cardioprotection. EBioMedicine. 2020; 57: 102884. https://doi.org/10.1016/j.ebiom.2020.102884.

[8] Mui D, Zhang Y. Mitochondrial scenario: roles of mitochondrial dynamics in acute myocardial ischemia/reperfusion injury. Journal of Receptor and Signal Transduction Research. 2021; 41: 1–5. https://doi.org/10.1080/10799893.2020.1784938.

[9] Zhang H, Hu H, Zhai C, Jing L, Tian H. Cardioprotective Strategies After Ischemia-Reperfusion Injury. American Journal of Cardiovascular Drugs: Drugs, Devices, and other Interventions. 2024; 24: 5–18. https://doi.org/10.1007/s40256-023-00614-4.

[10] Hausenloy DJ, Chilian W, Crea F, Davidson SM, Ferdinandy P, Garcia-Dorado D, *et al*. The coronary circulation in acute myocardial ischaemia/reperfusion injury: a target for cardioprotection. Cardiovascular Research. 2019; 115: 1143–1155. https://doi.org/10.1093/cvr/cvy286.

[11] Zhou M, Yu Y, Luo X, Wang J, Lan X, Liu P, *et al*. Myocardial Ischemia-Reperfusion Injury: Therapeutics from a Mitochondria-Centric Perspective. Cardiology. 2021; 146: 781–792. https://doi.org/10.1159/000518879.

[12] Ni H, Ou Z, Wang Y, Liu Y, Sun K, Zhang J, *et al*. XBP1 modulates endoplasmic reticulum and mitochondria crosstalk via regulating NLRP3 in renal ischemia/reperfusion injury. Cell Death Discovery. 2023; 9: 69. https://doi.org/10.1038/s41420-023-01360-x.

[13] Missiroli S, Patergnani S, Caroccia N, Pedriali G, Perrone M, Previati M, *et al*. Mitochondria-associated membranes (MAMs) and inflammation. Cell Death & Disease. 2018; 9: 329. https://doi.org/10.1038/s41419-017-0027-2.

[14] Yao H, Xie Y, Li C, Liu W, Yi G. Mitochondria-Associated Organelle Crosstalk in Myocardial Ischemia/Reperfusion Injury. Journal of Cardiovascular Translational Research. 2024; 17: 1106–1118. https://doi.org/10.1007/s12265-024-10523-9.

[15] Zhao WK, Zhou Y, Xu TT, Wu Q. Ferroptosis: Opportunities and Challenges in Myocardial Ischemia-Reperfusion Injury. Oxidative Medicine and Cellular Longevity. 2021; 2021: 9929687. https://doi.org/10.1155/2021/9929687.

[16] Yu X, Wang F, Liu H, Adams G, Aikhionbare F, Liu D, *et al*. ACAP4 protein cooperates with Grb2 protein to orchestrate epidermal growth factor-stimulated integrin β1 recycling in cell migration. The Journal of Biological Chemistry. 2011; 286: 43735–43747. https://doi.org/10.1074/jbc.M111.278770.

[17] Zhou W, Li X, Premont RT. Expanding functions of GIT Arf GTPase-activating proteins, PIX Rho guanine nucleotide exchange factors and GIT-PIX complexes. Journal of Cell Science. 2016; 129: 1963–1974. https://doi.org/10.1242/jcs.179465.

[18] Hashimoto S, Hashimoto A, Yamada A, Kojima C, Yamamoto H, Tsutsumi T, *et al*. A novel mode of action of an ArfGAP, AMAP2/PAG3/Papa lpha, in Arf6 function. The Journal of Biological Chemistry. 2004; 279: 37677–37684. https://doi.org/10.1074/jbc.M404196200.

[19] Stricker R, Reiser G. Functions of the neuron-specific protein ADAP1 (centaurin-α1) in neuronal differentiation and neurodegenerative diseases, with an overview of structural and biochem-

ical properties of ADAP1. Biological Chemistry. 2014; 395: 1321–1340. https://doi.org/10.1515/hsz-2014-0107.

[20] Kartopawiro J, Bower NI, Karnezis T, Kazenwadel J, Betterman KL, Lesieur E, *et al*. Arap3 is dysregulated in a mouse model of hypotrichosis-lymphedema-telangiectasia and regulates lymphatic vascular development. Human Molecular Genetics. 2014; 23: 1286–1297. https://doi.org/10.1093/hmg/ddt518.

[21] Song X, Liu W, Yuan X, Jiang J, Wang W, Mullen M, *et al*. Acetylation of ACAP4 regulates CCL18-elicited breast cancer cell migration and invasion. Journal of Molecular Cell Biology. 2018; 10: 559–572. https://doi.org/10.1093/jmcb/mjy058.

[22] Natsvlishvili N, Goguadze N, Zhuravliova E, Mikeladze D. Sigma-1 receptor directly interacts with Rac1-GTPase in the brain mitochondria. BMC Biochemistry. 2015; 16: 11. https://doi.org/10.1186/s12858-015-0040-y.

[23] Sha Z, Yang Y, Liu R, Bao H, Song S, Dong J, *et al*. Hepatic Ischemia-reperfusion Injury in Mice was Alleviated by Rac1 Inhibition - More Than Just ROS-inhibition. Journal of Clinical and Translational Hepatology. 2022; 10: 42–52. https://doi.org/10.14218/JCTH.2021.00057.

[24] Liu T, Juan Z, Xia B, Ren G, Xi Z, Hao J, *et al*. HSP70 protects H9C2 cells from hypoxia and reoxygenation injury through STIM1/IP3R. Cell Stress & Chaperones. 2022; 27: 535–544. https://doi.org/10.1007/s12192-022-01290-0.

[25] Wu MY, Yiang GT, Liao WT, Tsai APY, Cheng YL, Cheng PW, *et al*. Current Mechanistic Concepts in Ischemia and Reperfusion Injury. Cellular Physiology and Biochemistry: International Journal of Experimental Cellular Physiology, Biochemistry, and Pharmacology. 2018; 46: 1650–1667. https://doi.org/10.1159/000489241.

[26] Qian Q, Xie Y. Propofol protects H9C2 cells against hypoxia/reoxygenation injury through miR-449a and NR4A2. Experimental and Therapeutic Medicine. 2021; 22: 1181. https://doi.org/10.3892/etm.2021.10615.

[27] Fang Z, Miao Y, Ding X, Deng H, Liu S, Wang F, *et al*. Proteomic identification and functional characterization of a novel ARF6 GTPase-activating protein, ACAP4. Molecular & Cellular Proteomics: MCP. 2006; 5: 1437–1449. https://doi.org/10.1074/mcp.M600050-MCP200.

[28] Okabe H, Furukawa Y, Kato T, Hasegawa S, Yamaoka Y, Nakamura Y. Isolation of development and differentiation enhancing factor-like 1 (DDEFL1) as a drug target for hepatocellular carcinomas. International Journal of Oncology. 2004; 24: 43–48.

[29] Ma H, Guo X, Cui S, Wu Y, Zhang Y, Shen X, *et al*. Dephosphorylation of AMP-activated protein kinase exacerbates ischemia/reperfusion-induced acute kidney injury via mitochondrial dysfunction. Kidney International. 2022; 101: 315–330. https://doi.org/10.1016/j.kint.2021.10.028.

[30] Meurer M, Höcherl K. Renal ischemia-reperfusion injury impairs renal calcium, magnesium, and phosphate handling in mice. Pflugers Archiv: European Journal of Physiology. 2019; 471: 901–914. https://doi.org/10.1007/s00424-019-02255-6.

[31] Wu L, Huang WQ, Yu CC, Li YF. Moderate Hydrogen Peroxide Postconditioning Ameliorates Ischemia/Reperfusion Injury in Cardiomyocytes via STAT3-Induced Calcium, ROS, and ATP Homeostasis. Pharmacology. 2021; 106: 275–285. https://doi.org/10.1159/000511961.

[32] Iurova E, Rastorgueva E, Beloborodov E, Pogodina E, Fomin A, Sugak D, *et al*. Protective Effect of Peptide Calcium Channel Blocker Omega-Hexatoxin-Hv1a on Epithelial Cell during Ischemia-Reperfusion Injury. Pharmaceuticals (Basel, Switzerland). 2023; 16: 1314. https://doi.org/10.3390/ph16091314.

[33] Chang Y, Wang C, Zhu J, Zheng S, Sun S, Wu Y, *et al*. SIRT3 ameliorates diabetes-associated cognitive dysfunction via regulating mitochondria-associated ER membranes. Journal of Translational Medicine. 2023; 21: 494. https://doi.org/10.1186/s12967-023-04246-9.

[34] Zhang Z, Zhou H, Gu W, Wei Y, Mou S, Wang Y, *et al*. CGI1746 targets σ_1R to modulate ferroptosis through mitochondria-associated membranes. Nature Chemical Biology. 2024; 20: 699–709. https://doi.org/10.1038/s41589-023-01512-1.

[35] Barazzuol L, Giamogante F, Calì T. Mitochondria Associated Membranes (MAMs): Architecture and physiopathological role. Cell Calcium. 2021; 94: 102343. https://doi.org/10.1016/j.ceca.2020.102343.

[36] Qian J, Li Y, Yao H, Tian H, Wang H, Ai L, *et al*. ASAP3 regulates microvilli structure in parietal cells and presents intervention target for gastric acidity. Signal Transduction and Targeted Therapy. 2017; 2: 17003. https://doi.org/10.1038/sigtrans.2017.3.

[37] Liang J, Oyang L, Rao S, Han Y, Luo X, Yi P, *et al*. Rac1, A Potential Target for Tumor Therapy. Frontiers in Oncology. 2021; 11: 674426. https://doi.org/10.3389/fonc.2021.674426.

[38] Liang H, Huang J, Huang Q, Xie YC, Liu HZ, Wang HB. Pharmacological inhibition of Rac1 exerts a protective role in ischemia/reperfusion-induced renal fibrosis. Biochemical and Biophysical Research Communications. 2018; 503: 2517–2523. https://doi.org/10.1016/j.bbrc.2018.07.009.

[39] Han S, Li X, Xia N, Zhang Y, Yu W, Li J, *et al*. Myeloid Trem2 Dynamically Regulates the Induction and Resolution of Hepatic Ischemia-Reperfusion Injury Inflammation. International Journal of Molecular Sciences. 2023; 24: 6348. https://doi.org/10.3390/ijms24076348.

[40] Wang Y, Jian Y, Zhang X, Ni B, Wang M, Pan C. Melatonin protects H9c2 cardiomyoblasts from oxygen-glucose deprivation and reperfusion-induced injury by inhibiting Rac1/JNK/Foxo3a/Bim signaling pathway. Cell Biology International. 2022; 46: 415–426. https://doi.org/10.1002/cbin.11739.

[41] Kahles T, Luedike P, Endres M, Galla HJ, Steinmetz H, Busse R, *et al*. NADPH oxidase plays a central role in blood-brain barrier damage in experimental stroke. Stroke. 2007; 38: 3000–3006. https://doi.org/10.1161/STROKEAHA.107.489765.

[42] Dougherty CJ, Kubasiak LA, Frazier DP, Li H, Xiong WC, Bishopric NH, *et al*. Mitochondrial signals initiate the activation of c-Jun N-terminal kinase (JNK) by hypoxia-reoxygenation. FASEB Journal: Official Publication of the Federation of American Societies for Experimental Biology. 2004; 18: 1060–1070. https://doi.org/10.1096/fj.04-1505com.

[43] Mao X, Fan C, Yu X, Chen B, Jin F. DDEFL1 correlated with Rho GTPases activity in breast cancer. Oncotarget. 2017; 8: 112487–112497. https://doi.org/10.18632/oncotarget.22095.